ACS EARTH AND SPACE CHEMISTRY

http://pubs.acs.org/journal/aesccq

Article

Ozonolysis Chemistry and Phase Behavior of 1-Octen-3-ol-Derived Secondary Organic Aerosol

Kevin B. Fischer, Clarissa S. Gold, Rebecca M. Harvey, Adam N. Petrucci, and Giuseppe A. Petrucci*

Cite This: https://dx.doi.org/10.1021/acsearthspacechem.0c00092

Read Online

ACCESS | Metrics & More | Article Recommendations | Supporting Information

ABSTRACT: Secondary organic aerosol (SOA) is ubiquitous in the atmosphere and plays important roles in environmental chemical processes, influencing air quality and the Earth's radiative budget. In the present work, 1-octen-3-ol (OTL) was identified as one of several prominent green leaf volatiles (GLVs) emitted as a result of sugarcane wounding. GLVs, a subset of volatile organic compounds (VOCs), act as SOA precursors and are a potentially underrepresented source of the overall SOA budget. Here, ozonolysis experiments of OTL standards were carried out in Teflon chambers in conjunction with a scanning mobility particle sizer (SMPS), an electrical low pressure impactor (ELPI+), and a near-infrared laser desorption ionization aerosol mass spectrometer (NIR-LDI-AMS). Under our experimental conditions, the OTL ozonolysis rate constant and aerosol yield were estimated to be $5.00 \pm 0.58 \times 10^{-24}$ cm^3 s^{-1} molecule^{-1} and $1.03 \pm 0.07\%$, respectively. Bounce factor (BF) calculations based on the ELPI+ data at relative humidity (RH) levels of 5, 30, 60, and 90% suggest that the OTL-derived SOA exhibits largely non-liquid characteristics regardless of RH levels at particle genesis. Furthermore, high RH at particle genesis also appears to decrease the hygroscopicity of the SOA, impacting its ability to activate as cloud droplets. Online chemical analysis of the SOA using a NIR-LDI-AMS supports the production of oxygenated products ranging from 45 to 161 m/z, in addition to prominent oligomers well beyond this m/z range.

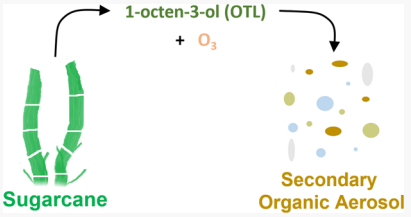

KEYWORDS: *green leaf volatile, secondary organic aerosol, sugarcane, bounce factor, aerosol mass spectrometer, cis-3-hexenol, cis-3-hexenyl acetate, 1-octen-3-ol*

INTRODUCTION

Atmospheric aerosols play essential roles in climatic processes, including participation in heterogeneous chemical reactions and affecting the distribution, abundance, and transport of trace gases.[1,2] Atmospheric aerosols furthermore influence the Earth's radiative budget by absorbing and scattering radiation (the direct effect)[3] and by acting as cloud condensation/ice nuclei (the indirect effect),[4,5] which themselves absorb/scatter radiation and also contribute to local weather phenomena.[6]

Organic aerosols (OAs) in particular contribute 20−50% to the total fine particle mass at continental midlatitudes, while in tropical forested areas contributions reach up to 90%.[7−9] More importantly, the majority of OAs (70−90%) is secondary in nature (SOA), having been produced by the gas-phase oxidation of volatile organic compounds (VOCs) present in the atmosphere.[10,11] While important strides have been made in better understanding SOA, many of the fundamental processes governing the formation, growth, and chemical and physical properties are still poorly understood. In fact, recent estimates of global SOA production rates suggest that important SOA precursors are still unidentified and that there remains a poor understanding of the chemical processes leading to SOA.[12−15] This lack of understanding also likely contributes to discrepancies between model predictions and the observed atmospheric aerosol content.[16]

One approach to identify VOCs acting as SOA precursors involves identifying land uses that cover large areas followed by characterization of volatile emissions and resulting SOAs formed from oxidation of these emissions.[17] For example, previous work has identified specific green leaf volatiles (GLVs), a subset of VOCs, emitted by turf grasses and probed the subsequent SOA products formed via ozonolysis.[17] However, many other potential GLV sources and their contribution to atmospheric aerosols remain largely unexplored.

The hand harvesting of sugarcane often involves a preharvest burn that produces a large amount of smoke, which is a major source of primary organic aerosol (POA).[18−22] Regarding SOA, Chang et al.[23] characterized the emissions of sugarcane extract and found that the predominant emissions were isoprene and monoterpenes and that about 30% of the emissions were other VOCs. The additional VOCs have yet to be characterized and may contain additional SOA precursors. The volatile emissions released during the preharvest burn and

Received: April 9, 2020
Revised: May 22, 2020
Accepted: June 1, 2020
Published: June 1, 2020

the harvesting of sugarcane itself, however, have not been characterized. Thus, the potential contribution of these GLVs to SOA has, to the best of our knowledge, not been evaluated.

Sugarcane is a C_4 plant in the *Poaceae* genus[24] and is expected to have emission profiles dominated by GLVs.[25] Sugarcane covers a vast area of land: 70 million acres globally and nearly 1 million acres in the US alone.[26] As a tropical plant, sugarcane is harvested during dry and sunny weather during hurricane and typhoon free months.[27] Additionally, tropospheric ozone is often present at elevated concentrations on sunny days.[28,29] The GLV emission potential, large land area coverage, and presence of ozone together suggest that sugarcane growing and harvesting related activities may contribute significantly to regional SOA.

In the present study, a GLV emission profile was measured for wounded sugarcane leaves and found to be composed primarily of *cis*-3-hexenyl acetate (CHA), *cis*-3-hexen-1-ol (HXL), and 1-octen-3-ol (OTL). Chemical mechanisms of SOA formation and yields by ozonolysis of CHA and HXL ozonolysis have been previously investigated.[17,30−32] Importantly, the reported SOA yields were of the same order as those of prominent atmospheric terpenes, such as α-pinene and limonene. Therefore, the current report focuses on OTL and the chemistry behind its subsequent ozonolysis and SOA formation. The SOA contribution of OTL is reported via chemical characterization, utilizing a near-infrared laser desorption/ionization aerosol mass spectrometer (NIR-LDI-AMS), and bounce factor (BF, a surrogate for particle viscosity) determination, utilizing an electrical low pressure impactor (ELPI+). Additionally, a mechanistic pathway for the formation of multigenerational OTL-derived SOA products is proposed and an approximate SOA yield and ozonolysis rate constant are reported.

MATERIALS AND METHODS

In all experiments, ozone was produced with a commercial generator (OL80A/DLS, Ozone Lab, Burton, BC, Canada) using dry, particle-free air. Ozone was injected by diverting the output flow of the generator to the chamber for a predetermined time pulse to yield the desired ozone concentration. Typical injection pulses were in the range of 10−35 s.

Two Teflon reaction chambers were utilized separately for this work and are referred to as the 775 L chamber and the 8 m^3 University of Vermont Environmental Chamber (UVMEC).[33] For both types of reaction chambers, dry zero air was used for flushing (after H_2O_2 passivation with UV lamps) until background aerosol mass and number concentrations were well below 0.01 $\mu g\ m^{-3}$ and 10 particles cm^{-3}, respectively. A glass microsyringe was used to quantitatively transfer GLV aliquots into a glass three-neck flask that was placed in a hot water bath. The liquid phase GLV content within the flask was visually monitored as a flow of dry zero air carried the newly volatilized GLV into the reaction chamber. Once all gaseous GLV was introduced, the dry zero air flow was shut off (typically after 10−20 min). The three-neck flask was sealed except for the dry zero air inlet and an outlet leading directly to the reaction chamber. All experiments were conducted under ambient temperature and atmospheric pressure. Particle size distributions were measured using a scanning mobility particle sizer (SMPS 3082, TSI Inc., Shoreview, MN, USA) operating with sheath and aerosol flows of 10 and 1.0 L min^{-1}, respectively.

GLV Emissions and Subsequent Ozonolysis. Sugarcane samples were collected by the University of Central Florida, Everglades Research and Education Center and stored in plastic oven bags. For all experiments, sugarcane samples were shipped to the University of Vermont overnight and analysis was performed within 24−36 h of harvest.

A measured mass of sugarcane leaves was placed inside the 775 L Teflon reaction chamber and GLV emissions were collected using solid phase microextraction (SPME), which consists of a polymer-coated fiber (65 μm PDMS/DVB, Sigma Aldrich) to which VOCs adsorb. Calibration, sample equilibration time, and method validation are described in SI-1. A sampling port located adjacent to the headspace area of the chamber allowed for easy and fast swapping of SPME sampling fibers. After a suitable collection time (which was determined to be 40 min, as described in SI-1), the fiber was extracted from the sample headspace and injected directly into the heated injection port (200 °C) of a gas chromatograph (GC, Clarus 600, PerkinElmer) equipped with an analytical column (Stabilwax 30 m, 0.32 mm i.d., Restek) and a mass spectrometer (MS, Clarus 600 T PerkinElmer) for chemical analysis.[34−36] The GC oven was programmed as follows: hold at 120 °C for 2 min, increase 10 °C min^{-1} to a final temperature of 220 °C and hold for 10 min. The total run time per sample was 22 min. The head pressure of the helium carrier gas was 1.8 psi, which resulted in a flow rate of 1.52 mL min^{-1}. Electron impact ionization (70 eV) was used and masses were scanned from 15 to 300 *m/z*. Chromatographic peaks were identified by spectral matching with the NIST 2005 mass spectral library and confirmed by comparison of retention times to those of known standards (where available). Standards of HXL, CHA, OTL, 2-hexenal, heptanal, and nonanal were purchased from Sigma-Aldrich, while decanal was purchased from Pfaltz & Bauer. All standards were reported as ≥95% pure and used without further purification.

OTL Ozonolysis Rate Constant. The ozonolysis rate constant (k) was estimated using an OTL standard according to a previously established method.[37,38] Briefly, the rate of ozone decay was measured in the presence of at least a 10-fold initial molar excess of OTL (to ensure pseudo-first order conditions). The OTL standard was added to the 775 L chamber first followed by ozone, which was added at a constant flow rate over a course of 30 s. Ozone concentration was monitored at 5 s intervals with an American Ecotech Serinus O_3 Monitor (model E020010). The loss of ozone and GLVs (i.e., the volatile SOA precursors) to chamber walls was found to be negligible over the time scale of previous kinetic experiments,[17] confirming that the reaction with OTL was the only significant removal process for ozone.

OTL-Derived SOA Yield. To estimate the SOA yield (% Y), standards of OTL were injected into the 8 m^3 UVMEC followed by ozone. The consumption of OTL and production of SOAs were then monitored and the SOA yield was calculated according to eq 1, where Δ[SOA] is the maximum SOA concentration ($\mu g\ m^{-3}$) generated and Δ[GLV] is the total amount of GLV consumed ($\mu g\ m^{-3}$) at that SOA maximum:

$$\%Y = \frac{\Delta[\mathrm{SOA}]}{\Delta[\mathrm{GLV}]} \times 100\% \quad (1)$$

The aerosol mass yields reported were determined at GLV and ozone mixing ratios of 200 ppb.

https://dx.doi.org/10.1021/acsearthspacechem.0c00092
ACS Earth Space Chem. XXXX, XXX, XXX−XXX

OTL-Derived SOA: Composition and Proposed Chemical Mechanism. Chemical analysis of SOA was carried out using a custom built near-infrared laser desorption/ionization aerosol mass spectrometer (NIR-LDI-AMS).[33,39] In this method, the OTL-derived SOA was sampled from the chamber following ozonolysis of the previously introduced OTL standard. Sampling occurred through a Liu-type aerodynamic lens and SOA was collimated into a particle beam that was aligned to deposit aerosol mass onto the surface of an aluminum probe (99.9% purity, ESPI metals, Ashland, OR) suspended under high vacuum. The aerosol collected on the probe's surface was both desorbed and ionized using an unfocused 3 mm diameter ND: YAG laser (Brio, Quantel USA, Big Sky, CO,) pulse with 4 ns half-width and 20 mJ energy. The deposited SOA mass was entirely desorbed by 2−3 laser shots. A time-of-flight mass analyzer was used for ion detection with a working mass range from 0 to 500 m/z and a mass resolution of 1000 at 300 m/z. Mass spectra were collected at 1−5 min intervals over the course of approximately 90 min. Mass spectra (from multiple laser shots) for a given time point were summed and normalized to the 145 m/z base peak.

OTL-Derived SOA: Bounce Factor. Bounce factor (BF) experiments required the use of the UVMEC due to the inherent high volume sampling rate (10 L min^{-1}). Following the OTL standard introduction into the UVMEC, ozone was introduced as described above. The particle BF method described previously[40] was utilized to infer the SOA phase state. Briefly, an electrical low pressure impactor (ELPI+, Dekati, Kangasala, Finland) operating sequentially with smooth (favoring bounce) and sintered (minimizing bounce) impaction plates was used to estimate the SOA bounce factor (BF) based on corrected current distributions generated by charged particles. Proprietary software provided by the instrument manufacturer applied a correction algorithm correcting for diffusion and space charger losses.[41,42] The BF was calculated according to eq 2:

$$\text{Bounce Factor(BF)} = \frac{I^{(\text{bounce})}_{\text{Filter Smooth}} - I^{(\text{no bounce})}_{\text{Filter Sintered}}}{\sum^{(\text{no bounce})}_{\text{Impactor Stage} > \text{Filter}}} \quad (2)$$

where $I^{(\text{bounce})}_{\text{filter (smooth)}}$ and $I^{(\text{no bounce})}_{\text{filter (sintered)}}$ are the corrected currents measured at the filter stage (i.e., the smallest diameter channel) of the smooth and sintered plates, respectively. $\sum I^{(\text{no bounce})}_{(\text{impactor stage}>\text{filter})}$ is the sum of the corrected currents obtained from all stages of the sintered plates except the filter stage. Sequential experiments, where smooth plates were first used followed by sintered plates and vice versa, were conducted under identical conditions and experimental parameters.

Experimental Conditions. Experimental conditions are summarized in Table 1. SOA mass loading (C_{SOA}) values obtained from SMPS measurements have been corrected for particle wall losses using ammonium sulfate in accordance with a previously established method.[43] All experiments were conducted in duplicate.

RESULTS AND DISCUSSION

An underestimation in model SOA production may be a result of a still incomplete understanding of SOA forming mechanisms and/or the omission of significant SOA precursors. C-4 plants, such as sugarcane, are known to emit GLVs (such as OTL) which produce SOA upon atmospheric processing. There is limited data on the role of OTL in atmospheric oxidation reactions[44,45] and we are not aware of any reports of its reaction with ozone to produce SOA. However, OTL has one terminal double bond (Scheme 1), which can react with ozone to form gas and particle phase products in addition to further multigenerational products.

Table 1. Experimental Conditions for All Experiments Performed[a]

	condition			
experiment	GLV mixing ratio (ppb)	ozone mixing ratio (ppb)	relative humidity (%)	SOA mass loading (C_{SOA}) ($\mu g\ m^{-3}$)
GLV emissions, ozonolysis*	N/A	800	20	1.6 ± 0.2
OTL-derived SOA: rate constant**	1000	100	5	N/A
OTL-derived SOA: yield**	200	200	5	10.8 ± 0.7
OTL-derived SOA: composition*	1000	1000	5	80 ± 4.4
OTL-derived SOA: bounce factor**	200	200	5, 30, 60, 90	1.3−5.0

[a]All experiments conducted under ambient temperature and atmospheric pressure. Experiments were conducted in 775 L chamber* or in 8 m^3 UVMEC**.

GLV Emissions and Subsequent Ozonolysis. A representative chromatogram (Figure 1) of sugarcane emissions before (A) and after (B) the injection of ozone gives a qualitative overview of the GLVs emitted and their consumption following ozonolysis. Post-ozonolysis data points are presented as negative values to allow for easy comparison to pre-ozonolysis data. The absolute value of the magnitude of the total ion chromatogram (TIC) intensity is therefore of importance. The dominant emissions include HXL and 2-hexenal, with lesser amounts of OTL, CHA, 3-hexenal, 1-heptanal, and toluene. While more commonly derived from anthropogenic sources, toluene has been identified as a potentially prominent GLV as well.[46,47] Additional chromatographic peaks are present but cannot be seen on the scale shown in Figure 1. All identified GLV emissions observed are listed in Table 2.

The reaction profiles for CHA, HXL, and OTL are shown in Figure 2, where ozone was injected 160 min following wounding of approximately 130 g of sugarcane (wet weight), which was freshly cut into 5−8 cm pieces. The pre-ozonolysis mixing ratio and emission rate for CHA was 62 ppb and 1.22 ± 0.18 $\mu g\ h^{-1}$ per gram sugarcane, and the corresponding values for HXL were 40 ppb and 0.6 ± 0.1 $\mu g\ h^{-1}$ per gram sugarcane. While an accurate calibration of OTL was not possible due to relatively small signal intensities for the SPME setup, a qualitative examination of Figure 1 suggests that the OTL pre-ozonolysis mixing ratio was below that of CHA and HXL. Therefore, each GLV data set was normalized to its base peak area to allow for easier comparison, as raw peak areas for each compound scaled several orders of magnitude. CHA and HXL data are presented as well to place OTL results into context (Figure 2). Previous CHA and HXL ozonolysis investigations, where a similar experimental approach and setup was utilized and where gaseous wall losses were found to be negligible, confirmed SOA production via a combination of SMPS, ELPI +, and NIR-LDI-AMS data.[17,31,32] As is evident from Figure 2,

https://dx.doi.org/10.1021/acsearthspacechem.0c00092
ACS Earth Space Chem. XXXX, XXX, XXX−XXX

Scheme 1. Proposed Abbreviated Reaction Mechanism for OTL Ozonolysis as Performed in Chamber Experiments. Boxed Products Appear in Mass Spectrum (Figure 3)

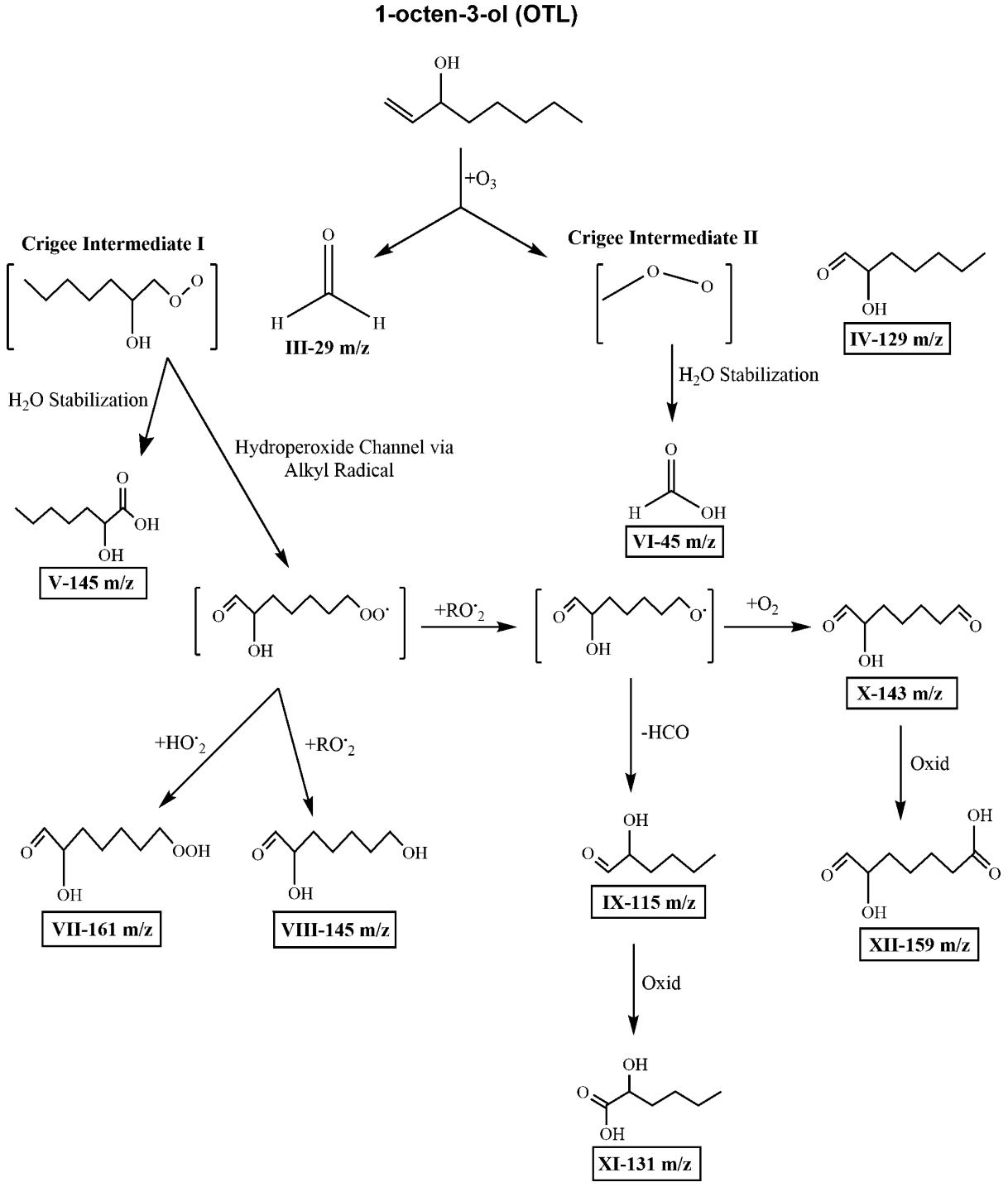

GLV mixing ratios for all three SOA precursors decreased following ozone injection. This is in line with the current knowledge regarding gas-phase ozonolysis, whereby alkenes are highly susceptible to oxidative cleavage along an unsaturated carbon bond.[48] This also mirrors the results reported previously for CHA and HXL.[17,30] While OTL is not, based on the work reported here, the dominant GLV emitted following sugarcane harvesting activities, it is still an unreported GLV that readily participates in ozonolysis, the reaction of which has previously not been reported.

OTL-Derived SOA: Rate Constant and Yield. The ozonolysis rate constant (k) of OTL was estimated using established methods[37,38] to be $5.00 \pm 0.58 \times 10^{-24}$ cm^3 s^{-1} molecule^{-1}. As a point of comparison, the rate constant of OTL with OH radicals (another atmospherically relevant oxidant) has, to the best of our knowledge, not been probed. However, the rate constant for OH with other relevant GLVs such as CHA and HXL has been estimated as 6.1×10^{-11} and 6.3×10^{-11} cm^3 s^{-1} molecule^{-1}, respectively,[49] which is several orders of magnitude higher than ozonolysis ($5.8 \pm 0.1 \times 10^{-17}$ and $5.8 \pm 0.9 \times 10^{-17}$ cm^3 s^{-1} molecule^{-1} for CHA and HXL,

https://dx.doi.org/10.1021/acsearthspacechem.0c00092
ACS Earth Space Chem. XXXX, XXX, XXX−XXX

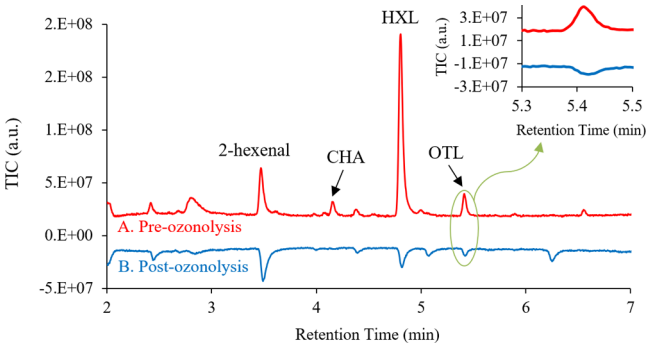

Figure 1. Chromatograms of sugarcane emissions (A) before ozonolysis, where strong signals from CHA, HXL, OTL, and 2-hexenal are observed, and (B) after ozonolysis. Negative values used for post-ozonolysis data to allow for easy comparison with pre-ozonolysis data.

Table 2. GLV Emissions from Sugarcane and Subsequent Ozonolysis Products[a]

emission	retention time (min)	product	retention time (min)
toluene	2.3	methyl ester butanoic acid	2.7
3-hexenal	2.8	heptanal	3.1
2-hexenal	3.5	octanal	4.0
cis-3-hexenyl acetate (CHA)	4.2	nonanal	5.1
cis-3-hexen-1-ol (HXL)	4.8	decanal	6.2
1-octene-3-ol (OTL)	5.4		

[a]Compounds were identified by comparison to the NIST spectral library.

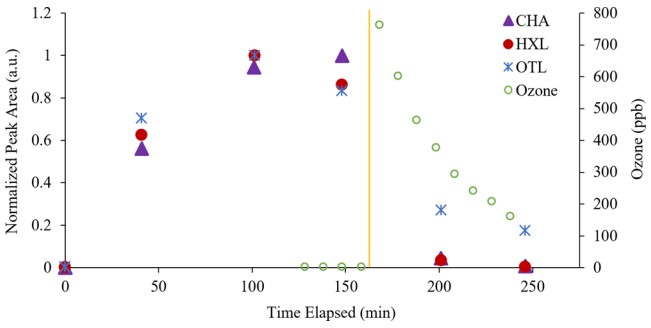

Figure 2. GLV emissions from 130 g (wet weight) of wounded sugarcane. After 160 min, 800 ppb ozone was injected. Maximum C_{SOA} observed = 1.6 ± 0.2 μg m^{-3}. The vertical line delineates GLV production (left) from GLV consumption (right).

respectively),[30] indicating a faster reaction under OH conditions compared to ozonolysis conditions. This is commonly observed with terpenes such as α-pinene as well.[50,51] Nonetheless, the reaction with ozone is a significant atmospheric sink for terpenes[52] and this is expected to be the case for OTL as well.

To determine the SOA forming potential of OTL, its aerosol yield (%Y) was estimated using standards of OTL in accordance with eq 1. The aerosol mass yield for OTL at 200 ppb was found to be 1.03 ± 0.07%, which is slightly lower but of the same order of magnitude as other GLVs such as CHA and HXL.[17,53] It is important to note that this comparison to CHA and HXL is based on studies that utilized higher GLV and ozone mixing ratios. Generally, elevated mixing ratios inherently lead to higher aerosol yields due to increased semivolatile gas to particle partitioning stemming from a higher total condensed mass.[54] Therefore, it must be stressed that the aerosol yield measured in these experiments is only an estimate specific to the GLV and O_3 mixing ratios used here. It is well known that the aerosol yield is a strong function of overall organic mass loading, among other parameters, and therefore it is not possible to simply extrapolate the measured yield. Also, gas to wall partitioning of semivolatile and low volatility oxidized products, which has been well documented for Teflon chambers,[55−57] may artificially lower the measured SOA yields.[58] Nonetheless, the results presented herein suggest strongly that ozonolysis of GLVs from C-4 plants, and OTL specifically, constitute potentially significant sources of regional SOA, which is in addition to GLVs from other biogenic sources.

OTL-Derived SOA: Composition and Proposed Chemical Mechanism. NIR-LDI-AMS spectra of OTL-derived SOA were collected following ozonolysis of OTL standards. A normalized spectrum, based on all collected spectra for the entire experimental run, was generated, which depicts the desorbed and ionized mass (Figure 3).

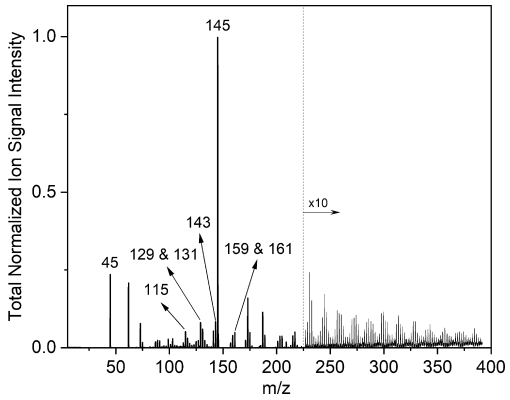

Figure 3. Representative normalized NIR-LDI-AMS spectrum based on collection of spectra over a course of 56 min. Normalization occurred after summation of individual m/z values collected for each spectrum. Maximum C_{SOA} of 80 ± 4.4 μg m^{-3}. OTL (5 μL) (corresponding to 1000 pbb) was injected into the 775 L Teflon reaction chamber followed by 1000 ppb of ozone.

A proposed mechanism for the ozonolysis of OTL was developed to describe the formation of oxygenated products ranging from 45−161 m/z (Scheme 1). It should be noted that other relevant oxidants, such as OH radicals, are expected to participate in the oxidation of OTL, leading to the subsequent formation of SOA (among other products). That is, besides the oxidation pathways presented here, there are other oxidation pathways worth exploring that warrant future work.

Mass spectral evidence suggests that the ozonolysis pathway for OTL oxidation is similar to that observed for CHA and HXL.[31] A detailed description of the ozonolysis mechanisms for these GLVs and other alkenes are discussed in depth elsewhere.[59,60] In brief, oxidation begins with the addition of ozone across the terminal double bond of OTL, leading to the formation of a primary ozonide that readily fragments to form two Criegee intermediates (CI-I and CI-II) and two oxidized primary products (III and IV).

https://dx.doi.org/10.1021/acsearthspacechem.0c00092
ACS Earth Space Chem. XXXX, XXX, XXX−XXX

The Criegee intermediates can engage in multigenerational chemistry via several channels of reactivity, including bimolecular reactions with water and further oxidation of CI-I through a hydroperoxide channel.[61,62] In instances of bimolecular reactions with water, CI-I and CI-II form products V and VI, respectively, which possess a low enough vapor pressure to be observed in the particle phase. It is also known that Criegee intermediates react with acids of a suitable strength to form organic peroxides. In the aforementioned hydroperoxide channel, CI-I rearranges to form a hydroperoxide that decomposes to form both a hydroxyl and alkyl radical (not shown in Scheme 1). The alkyl radical subsequently reacts with molecular oxygen to from an alkylperoxy that may participate in additional reactions with other radical species, such as $HO\bullet_2$ and $RO\bullet_2$, to form a secondary generation of low volatility products, including VII and VIII.[62]

Previous work has identified NO as a pertinent reactant in alkene oxidation.[63] However, it is not expected to play a significant role for ozonolysis experiments presented here, as background NO mixing ratios are in the parts per trillion range[64,65] and NO reacts rapidly with O_3.[43] The alkylperoxy originating from CI-I instead likely reacts with peroxy radicals ($RO_2\bullet$), creating an alkoxy species that can experience HCO abstraction and/or further oxidation by O_2 to yield low volatility and oxidized compounds, including products IX, X, XI, and XII.[17,59,62,66,67] It should be noted that NO mixing ratios have the potential to increase during sugarcane harvesting in the event of, but not limited to, heavy agricultural vehicle usage. Additionally, NO mixing ratios associated with sugarcane farms may vary spatially and temporally.[68] The potentially large variability of NO mixing ratios and its subsequent impact on OTL (and other GLVs) chemistry warrants additional work.

Formaldehyde (III) is expected to be found in the vapor phase but was not observed as a product. Given that SPME is efficient at sampling *semi*-VOCs; however, the high volatility of this compound may have limited our ability to sample and therefore detect/measure it. 2-hydroxyheptanoic acid, 2-hydroxyheptanal, and other secondary products however have sufficiently low vapor pressures (0.0349 and 4.57 Pa, as calculated by the EPA EPI database),[69] and they are expected to contribute to SOA. Additionally, the hydroxyl group in OTL is expected to participate in secondary oligomerization reactions that would lead to additional SOA mass.[31]

Prominent products were also measured beyond m/z 161, likely formed via accretion reactions. These reactions have not, to the best of our knowledge, been investigated for OTL-derived SOA specifically. However, previous studies have probed other prominent biogenic SOA precursors such as isoprene,[70] where oligomer formation following reactions with Criegee intermediates was shown to occur via various pathways, including: bimolecular reactions with gaseous water,[71] peroxy radicals,[72] and organic acids.[73] Oligomers produced as a result of alkene oxidation possess low saturation vapor pressures, allowing them to exist in the particle phase, thereby contributing to the tropospheric SOA budget.[74−77] Furthermore, oligomers have been shown to contribute to particle growth,[78] forming almost immediately after the start of the reaction and acting as an essential component in early stages of biogenic SOA formation and growth.[79] These oligomers are also expected to exhibit more solid-like properties,[80] which is supported by the BF data (next section) presented herein. As such, oligomers observed for OTL-derived SOA likely play an essential role in initial particle formation and subsequent growth and aging of OTL-derived SOA.

OTL-Derived SOA: Bounce Factor (BF). Elucidating the physical state of SOA can provide insights into SOA formation[81,82] and growth,[83] gas−particle partitioning,[84] reactive uptake on particle surfaces,[85,86] and ultimately atmospheric impacts.[87−89] Employing a previously established method,[40] the BF was determined for OTL-derived SOA generated under varying RH levels (Figure 4). This approach is

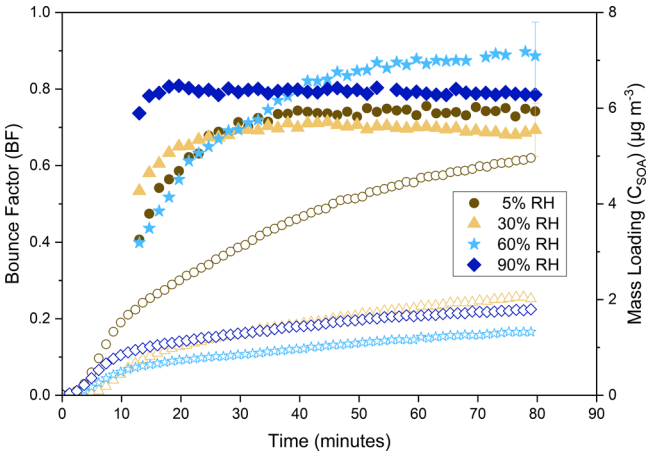

Figure 4. Bounce factor (BF, filled symbols) and mass loading (C_{SOA}, open symbols) of OTL-derived SOA. Ozone injection at time = 0, following introduction of 10 μL (200 ppb) OTL into the UVMEC. BF calculated from the ELPI data, and the C_{SOA} data obtained from SMPS measurements. Error bars represent ± 10%, based on estimates from previous work.[40]

in stark contrast to most reports in the literature where SOA is generated under dry conditions prior to studies of water and/or reactive gas uptake post-genesis.[86,90−93] Here, SOA particle generation was initiated via ozone injection into environments containing the SOA precursor at different relative humidity levels: 5% (dry), 30, 60, and 90% RH. Therefore, it is likely that the presence of water vapor impacted the chemical formation and evolution of the SOA,[94−96] as well as subsequent uptake of water vapor by particles.[97,98]

According to SMPS data, a sizeable portion of the initially generated SOA consisted of particles <10 nm in diameter, which overlaps with the cut off diameter (D_{50}) of the ELPI filter stage (6.0 nm).[40] The D_{50} corresponds to the specific particle diameter with a 50% collection efficiency. For the smooth impaction plates, these initially generated small particles would reach the filter stage due to their aerodynamic diameter, not bounce. The same would occur for the sintered plates. In accordance with eq 2, for the smooth plates, these particles would be treated as if they first bounced and then subsequently reached the filter stage. This would therefore lead to erroneously decreased BF. However, the particle size distribution swiftly shifts toward the higher diameter values as a function of experimental time. Therefore, the initial (time < 12 min) BF values have been omitted from Figure 4. For geometric mean diameter data, see Figure S5. Interestingly, SOA generated at higher RH did not exhibit decreased bounce, as one might posit if water vapor condensed onto the particles. Rather, a slightly increased bounce behavior was suggested

https://dx.doi.org/10.1021/acsearthspacechem.0c00092
ACS Earth Space Chem. XXXX, XXX, XXX−XXX

when particle genesis occurred under conditions of elevated RH as compared to dry conditions. However, statistical significance of the differences has not been evaluated at this point.

The SOA generated under humid conditions also do not appear to readily take up water, as suggested by the constant BF measured for 80 min following ozonolysis under 30 and 90% RH. In fact, under 60% RH, the BF continues to increase up to 80 min following ozonolysis. This suggests that SOA generated under humid conditions, at least for the case of OTL-derived SOA, may have lower hygroscopicity and may be less likely to be activated as cloud droplets. Taken together, these observations strongly suggest that the role of gaseous water at particle genesis not only impacts the SOA chemical profile but can have implications for subsequent gas uptake (be it water or other gases) by SOA during atmospheric aging.

All SOA generated under both dry and humid conditions demonstrated considerable particle bounce, which suggests that OTL-derived SOA remain non-liquid in nature.[40] This is contrary to conventional assumptions often used for atmospheric modeling in which the SOA mass is considered a liquid that undergoes instantaneous equilibrium partitioning with semivolatile organic compounds.[84,99] This does not appear to be limited to solely OTL-derived SOA, however. SOA derived from other VOCs, including but not limited to α-pinene, CHA, and HXL, have also exhibited non-liquid (including semisolid and solid) behavior under some conditions, such as low relative humidity.[32,81,100−102] In fact, our results are in accordance with a recent report that diffusion in α-pinene SOA remains appreciably slow even at 80% RH.[103] The non-liquid character implies higher viscosity, which has been shown to decrease theSOA growth rate due to lower molecular diffusion within the particle.[81,104] Furthermore, for a particle of higher viscosity, heterogeneous oxidation by O_3 is likely limited more to the surface of the particle as opposed to the particle bulk.[105] Additionally, the limited partitioning of SVOCs into larger, more viscous particles was recently found to instead promote preferential growth of smaller particles inherently possessing shorter diffusion time scales.[106] Therefore, due to its partial non-liquid character, multigenerational and aged OTL-derived SOA likely exhibit decreased growth rates and subsequently lower particle masses with limited heterogeneous O_3 oxidation (compared to low viscosity liquid particles), which may have subsequent ramifications for both direct (such as radiative forcing) and indirect (such as acting as cloud condensation nuclei) climate effects. These effects may be even more pronounced for OTL- derived SOA under conditions of lower mass loadings, where other relevant VOCs such as CHA, α-pinene, and limonene have been shown to exhibit a more non-liquid behavior.[32,107,108]

CONCLUSIONS

Alongside other prominent GLVs, OTL has been identified as a relevant GLV emitted following the harvesting and subsequent wounding of sugarcane. Ozonolysis of OTL standards led to the formation of SOA products possessing significant non-liquid behavior at all RH levels (5, 30, 60, and 90% RH) studied, which were present at particle genesis and held constant. In addition, the mass spectral data suggests the formation of oxygenated SOA ranging from 45 to 161 m/z in addition to prominent oligomers well beyond this m/z range. This has important implications for initial particle formation, subsequent growth, and aging, while emphasizing the need for additional work focusing on the fundamental chemical processes occurring at the molecular level during SOA production. Besides OTL, numerous other compounds, including CHA and HXL, were identified as prominent GLVs emitted as a direct result of sugarcane harvesting and further wounding. Furthermore, sugarcane emissions offer a prime system to study the dynamics of a mixed system, as sugarcane harvests have the potential to contribute POA simultaneously with SOA.

Results presented herein with regard to the SOA particle phase are in apparent stark contrast with the existing reports of water uptake by SOA from a number of precursors. In these previous reports, particle viscosity is typically shown to decrease at higher RH (i.e., decreasing particle bounce) to the point of deliquescence (i.e., particle bounce eliminated entirely, implying liquid particles).[86,90] The apparent discrepancy may be explained by the fact that in previous work, SOA was generated under dry conditions (typically with RH <5% and always <50%) and then subjected to varying relative humidity levels to measure water uptake. As such, the results presented here show clearly that RH at particle genesis plays a critical role in SOA aging, especially as it concerns water uptake, highlighting the continued need for laboratory studies that more accurately represent our atmosphere.

ASSOCIATED CONTENT

Supporting Information

The Supporting Information is available free of charge at https://pubs.acs.org/doi/10.1021/acsearthspacechem.0c00092.

Calibration and determination of sample (equilibration) time for SPME sampling of sugarcane emissions, determination of rate constant for OTL, and geometric mean diameter for SOA from BF experiments (PDF)

AUTHOR INFORMATION

Corresponding Author

Giuseppe A. Petrucci − *Department of Chemistry, The University of Vermont, Burlington, Vermont 05405, United States*; orcid.org/0000-0002-1241-6674; Email: giuseppe.petrucci@uvm.edu

Authors

Kevin B. Fischer − *Department of Chemistry, The University of Vermont, Burlington, Vermont 05405, United States*

Clarissa S. Gold − *Department of Chemistry, The University of Vermont, Burlington, Vermont 05405, United States*

Rebecca M. Harvey − *Department of Chemistry, The University of Vermont, Burlington, Vermont 05405, United States*

Adam N. Petrucci − *Department of Chemistry, The University of Vermont, Burlington, Vermont 05405, United States*

Complete contact information is available at: https://pubs.acs.org/10.1021/acsearthspacechem.0c00092

Notes

The authors declare no competing financial interest.

ACKNOWLEDGMENTS

We would like to thank Dr. Hardev Sandhu at the University of Central Florida, Everglades Research and Education Center for his assistance in acquiring sugarcane plants for analysis. We would also like to thank Dr. Molly Costanza-Robinson for her

help in establishing the SPME protocol. This material is based upon work supported by the National Science Foundation under Grants CHE-1213632 and CHE-1709751, as well as the Vermont NASA EPSCoR Graduate Research Assistantship under Program No. 025036.

REFERENCES

(1) Haywood, J.; Boucher, O. Estimates of the direct and indirect radiative forcing due to tropospheric aerosols: A review. *Rev. Geophys.* **2000**, *38*, 513−543.
(2) Andreae, M. O.; Crutzen, P. J. Atmospheric aerosols: Biogeochemical sources and role in atmospheric chemistry. *Science* **1997**, *276*, 1052−1058.
(3) Yu, H.; Kaufman, Y. J.; Chin, M.; Feingold, G.; Remer, L. A.; Anderson, T. L.; Balkanski, Y.; Bellouin, N.; Boucher, O.; Christopher, S.; DeCola, P.; Kahn, R.; Koch, D.; Loeb, N.; Reddy, M. S.; Schulz, M.; Takemura, T.; Zhou, M. A review of measurement-based assessments of the aerosol direct radiative effect and forcing. *Atmos. Chem. Phys.* **2006**, *6*, 613−666.
(4) Berkemeier, T.; Shiraiwa, M.; Pöschl, U.; Koop, T. Competition between water uptake and ice nucleation by glassy organic aerosol particles. *Atmos. Chem. Phys.* **2014**, *14*, 12513−12531.
(5) Scott, C. E.; Spracklen, D. V.; Pierce, J. R.; Riipinen, I.; D'Andrea, S. D.; Rap, A.; Carslaw, K. S.; Forster, P. M.; Artaxo, P.; Kulmala, M.; Rizzo, L. V.; Swietlicki, E.; Mann, G. W.; Pringle, K. J. Impact of gas-to-particle partitioning approaches on the simulated radiative effects of biogenic secondary organic aerosol. *Atmos. Chem. Phys.* **2015**, *15*, 12989−13001.
(6) Boucher, O.; Randall, D.; rtaxo, P.; Bretherton, C.; Feingold, G.; Forster, P.; Kerminen, V.-M.; Kondo, Y.; Liao, H.; Lohmann, U.; Rasch, P.; Satheesh, S. K.; Stevens, B.; Zhang, X. Y. *The Physical Science Basis. Contribution of Working Group I to the Fifth Assessment Report of the Intergovernmental Panel on Climate Change*; Cambridge, United Kingdom and New York, NY, USA, 2013.
(7) Jimenez, J. L.; Canagaratna, M. R.; Donahue, N. M.; Prevot, A. S. H.; Zhang, Q.; Kroll, J. H.; DeCarlo, P. F.; Allan, J. D.; Coe, H.; Ng, N. L.; Aiken, A. C.; Docherty, K. S.; Ulbrich, I. M.; Grieshop, A. P.; Robinson, A. L.; Duplissy, J.; Smith, J. D.; Wilson, K. R.; Lanz, V. A.; Hueglin, C.; Sun, Y. L.; Tian, J.; Laaksonen, A.; Raatikainen, T.; Rautiainen, J.; Vaattovaara, P.; Ehn, M.; Kulmala, M.; Tomlinson, J. M.; Collins, D. R.; Cubison, M. J.; Dunlea, J.; Huffman, J. A.; Onasch, T. B.; Alfarra, M. R.; Williams, P. I.; Bower, K.; Kondo, Y.; Schneider, J.; Drewnick, F.; Borrmann, S.; Weimer, S.; Demerjian, K.; Salcedo, D.; Cottrell, L.; Griffin, R.; Takami, A.; Miyoshi, T.; Hatakeyama, S.; Shimono, A.; Sun, J. Y.; Zhang, Y. M.; Dzepina, K.; Kimmel, J. R.; Sueper, D.; Jayne, J. T.; Herndon, S. C.; Trimborn, A. M.; Williams, L. R.; Wood, E. C.; Middlebrook, A. M.; Kolb, C. E.; Baltensperger, U.; Worsnop, D. R. Evolution of Organic Aerosols in the Atmosphere. *Science* **2009**, *326*, 1525−1529.
(8) Hallquist, M.; Wenger, J. C.; Baltensperger, U.; Rudich, Y.; Simpson, D.; Claeys, M.; Dommen, J.; Donahue, N. M.; George, C.; Goldstein, A. H.; Hamilton, J. F.; Herrmann, H.; Hoffmann, T.; Iinuma, Y.; Jang, M.; Jenkin, M. E.; Jimenez, J. L.; Kiendler-Scharr, A.; Maenhaut, W.; McFiggans, G.; Mentel, T. F.; Monod, A.; Prévôt, A. S. H.; Seinfeld, J. H.; Surratt, J. D.; Szmigielski, R.; Wildt, J. The formation, properties and impact of secondary organic aerosol: current and emerging issues. *Atmos. Chem. Phys.* **2009**, *9*, 5155−5236.
(9) Ehn, M.; Thornton, J. A.; Kleist, E.; Sipilä, M.; Junninen, H.; Pullinen, I.; Springer, M.; Rubach, F.; Tillmann, R.; Lee, B.; Lopez-Hilfiker, F.; Andres, S.; Acir, I.-H.; Rissanen, M.; Jokinen, T.; Schobesberger, S.; Kangasluoma, J.; Kontkanen, J.; Nieminen, T.; Kurtén, T.; Nielsen, L. B.; Jørgensen, S.; Kjaergaard, H. G.; Canagaratna, M.; Maso, M. D.; Berndt, T.; Petäjä, T.; Wahner, A.; Kerminen, V.-M.; Kulmala, M.; Worsnop, D. R.; Wildt, J.; Mentel, T. F. A large source of low-volatility secondary organic aerosol. *Nature* **2014**, *506*, 476−479.
(10) Kanakidou, M.; Seinfeld, J. H.; Pandis, S. N.; Barnes, I.; Dentener, F. J.; Facchini, M. C.; Van Dingenen, R.; Ervens, B.; Nenes, A.; Nielsen, C. J.; Swietlicki, E.; Putaud, J. P.; Balkanski, Y.; Fuzzi, S.; Horth, J.; Moortgat, G. K.; Winterhalter, R.; Myhre, C. E. L.; Tsigaridis, K.; Vignati, E.; Stephanou, E. G.; Wilson, J. Organic aerosol and global climate modelling: a review. *Atmos. Chem. Phys.* **2005**, *5*, 1053−1123.
(11) Shrivastava, M.; Easter, R. C.; Liu, X.; Zelenyuk, A.; Singh, B.; Zhang, K.; Ma, P.-L.; Chand, D.; Ghan, S.; Jimenez, J. L.; Zhang, Q.; Fast, J.; Rasch, P. J.; Tiitta, P. Global transformation and fate of SOA: Implications of low-volatility SOA and gas-phase fragmentation reactions. *J. Geophys. Res.: Atmos.* **2015**, *120*, 4169−4195.
(12) Goldstein, A. H.; Galbally, I. E. Known and unexplored organic constituents in the earth's atmosphere. *Environ. Sci. Technol.* **2007**, *41*, 1514−1521.
(13) Carlton, A. G.; Wiedinmyer, C.; Kroll, J. H. A review of Secondary Organic Aerosol (SOA) formation from isoprene. *Atmos. Chem. Phys.* **2009**, *9*, 4987−5005.
(14) Shilling, J. E.; Zaveri, R. A.; Fast, J. D.; Kleinman, L.; Alexander, M. L.; Canagaratna, M. R.; Fortner, E.; Hubbe, J. M.; Jayne, J. T.; Sedlacek, A.; Setyan, A.; Springston, S.; Worsnop, D. R.; Zhang, Q. Enhanced SOA formation from mixed anthropogenic and biogenic emissions during the CARES campaign. *Atmos. Chem. Phys.* **2013**, *13*, 2091−2113.
(15) Bruns, E. A.; El Haddad, I.; Slowik, J. G.; Kilic, D.; Klein, F.; Baltensperger, U.; Prévôt, A. S. H. Identification of significant precursor gases of secondary organic aerosols from residential wood combustion. *Sci. Rep.* **2016**, *6*, 27881.
(16) Tsui, W. G.; McNeill, V. F. Modeling Secondary Organic Aerosol Production from Photosensitized Humic-like Substances (HULIS). *Environ. Sci. Technol. Lett.* **2018**, *5*, 255−259.
(17) Harvey, R. M.; Zahardis, J.; Petrucci, G. A. Establishing the contribution of lawn mowing to atmospheric aerosol levels in American suburbs. *Atmos. Chem. Phys.* **2014**, *14*, 797−812.
(18) Chow, J. C.; Watson, J. G.; Lu, Z.; Lowenthal, D. H.; Frazier, C. A.; Solomon, P. A.; Thuillier, R. H.; Magliano, K. Descriptive analysis of PM2.5 and PM10 at regionally representative locations during SJVAQS/AUSPEX. *Atmos. Environ.* **1996**, *30*, 2079−2112.
(19) Godoi, R. H. M.; Godoi, A. F. L.; Worobiec, A.; Andrade, S. J.; de Hoog, J.; Santiago-Silva, M. R.; Van Grieken, R. Characterisation of sugar cane combustion particles in the Araraquara region, Southeast Brazil. *Microchim. Acta* **2004**, *145*, 53−56.
(20) Hall, D.; Wu, C.-Y.; Hsu, Y.-M.; Stormer, J.; Engling, G.; Capeto, K.; Wang, J.; Brown, S.; Li, H.-W.; Yu, K.-M. PAHs, carbonyls, VOCs and PM2.5 emission factors for pre-harvest burning of Florida sugarcane. *Atmos. Environ.* **2012**, *55*, 164−172.
(21) Lara, L.; Artaxo, P.; Martinelli, L.; Camargo, P.; Victoria, R.; Ferraz, E. Properties of aerosols from sugar-cane burning emissions in Southeastern Brazil. *Atmos. Environ.* **2005**, *39*, 4627−4637.
(22) Yokelson, R. J.; Christian, T. J.; Karl, T. G.; Guenther, A. The tropical forest and fire emissions experiment: laboratory fire measurements and synthesis of campaign data. *Atmos. Chem. Phys.* **2008**, *8*, 3509−3527.
(23) Chang, K. H.; Chen, T. F.; Huang, H. C. Estimation of biogenic volatile organic compounds emissions in subtropical island - Taiwan. *Sci. Total Environ.* **2005**, *346*, 184−199.
(24) Lakshmanan, P.; Geijskes, R. J.; Aitken, K. S.; Grof, C. L. P.; Bonnett, G. D.; Smith, G. R. Sugarcane biotechnology: The challenges and opportunities. *In Vitro Cell. Dev. Biol.: Plant* **2005**, *41*, 345−363.
(25) Clarke, M. A.; Godshall, M. A., Chemistry and Processing of Sugarbeet and Sugarcane. *Proceedings of the Symposium on the Chemistry and Processing of Sugarbeet, Denver, Colorado, April 6, 1987 and the Symposium on the Chemistry and Processing of Sugarcane, New Orleans, Louisiana, September 3−4, 1987*. Elsevier Science: 2013.
(26) Agriculture, U. D. O. *USDA 2012 Agriculture Report*; http://www.agcensus.usda.gov/Publications/2012/#full_report, 2012.
(27) Everingham, Y. L.; Muchow, R. C.; Stone, R. C.; Inman-Bamber, N. G.; Singels, A.; Bezuidenhout, C. N. Enhanced risk management and decision-making capability across the sugarcane industry value chain based on seasonal climate forecasts. *Agric. Syst.* **2002**, *74*, 459−477.

https://dx.doi.org/10.1021/acsearthspacechem.0c00092
ACS Earth Space Chem. XXXX, XXX, XXX−XXX

(28) Steinbrecher, R.; Klauer, M.; Hauff, K.; Stockwell, W. R.; Jaeschke, W.; Dietrich, T.; Herbert, F. Biogenic and anthropogenic fluxes of non-methane hydrocarbons over an urban-imapcted forest, Frankfurter Stadtwald, Germany. *Atmos. Environ.* **2000**, *34*, 3779−3788.
(29) Seinfeld, J. H.; Pandis, S. N., *Atmospheric Chemistry and Physics: From Air Pollution to Climate Change*; Wiley, 2016.
(30) Harvey, R. M.; Petrucci, G. A. Control of ozonolysis kinetics and aerosol yield by nuances in the molecular structure of volatile organic compounds. *Atmos. Environ.* **2015**, *122*, 188−195.
(31) Jain, S.; Zahardis, J.; Petrucci, G. A. Soft Ionization Chemical Analysis of Secondary Organic Aerosol from Green Leaf Volatiles Emitted by Turf Grass. *Environ. Sci. Technol.* **2014**, *48*, 4835−4843.
(32) Jain, S.; Fischer, K.; Petrucci, G. The Influence of Absolute Mass Loading of Secondary Organic Aerosols on Their Phase State. *Atmosphere* **2018**, *9*, 131.
(33) Geddes, S.; Nichols, B.; Flemer, S., Jr.; Eisenhauer, J.; Zahardis, J.; Petrucci, G. A. Near-Infrared Laser Desorption/Ionization Aerosol Mass Spectrometry for Investigating Primary and Secondary Organic Aerosols under Low Loading Conditions. *Anal. Chem.* **2010**, *82*, 7915−7923.
(34) Baker, B.; Sinnott, M. Analysis of sesquiterpene emissions by plants using solid phase microextraction. *J. Chromatogr. A* **2009**, *1216*, 8442−8451.
(35) Cornu, A.; Carnat, A.-P.; Martin, B.; Coulon, J.-B.; Lamaison, J.-L.; Berdagué, J.-L. Solid-Phase Microextraction of Volatile Components from Natural Grassland Plants. *J. Agric. Food Chem.* **2001**, *49*, 203−209.
(36) Bouvier-Brown, N. C.; Holzinger, R.; Palitzsch, K.; Goldstein, A. H. Quantifying sesquiterpene and oxygenated terpene emissions from live vegetation using solid-phase microextraction fibers. *J. Chromatogr. A* **2007**, *1161*, 113−120.
(37) Grosjean, D.; Grosjean, E.; Williams, E. L. Rate Constants for the Gas-Phase Reactions of Ozone with Unsaturated Alcohols, Esters, and Carbonyls. *Int. J. Chem. Kinet.* **1993**, *25*, 783−794.
(38) Grosjean, E.; Grosjean, D. Rate Constants for the Gas-Phase Reactions of Ozone with Unsaturated Aliphatic-Alcohols. *Int. J. Chem. Kinet.* **1994**, *26*, 1185−1191.
(39) Geddes, S.; Nichols, B.; Todd, K.; Zahardis, J.; Petrucci, G. A. Near-infrared laser desorption/ionization aerosol mass spectrometry for measuring organic aerosol at atmospherically relevant aerosol mass loadings. *Atmos. Meas. Tech.* **2010**, *3*, 1175−1183.
(40) Jain, S.; Petrucci, G. A. A New Method to Measure Aerosol Particle Bounce Using a Cascade Electrical Low Pressure Impactor. *Aerosol Sci. Technol.* **2015**, *49*, 390−399.
(41) Virtanen, A.; Marjamäki, M.; Ristimäki, J.; Keskinen, J. Fine particle losses in electrical low-pressure impactor. *J. Aerosol Sci.* **2001**, *32*, 389−401.
(42) Järvinen, A.; Aitomaa, M.; Rostedt, A.; Keskinen, J.; Yli-Ojanperä, J. Calibration of the new electrical low pressure impactor (ELPI+). *J. Aerosol Sci.* **2014**, *69*, 150−159.
(43) Presto, A. A.; Huff Hartz, K. E.; Donahue, N. M. Secondary Organic Aerosol Production from Terpene Ozonolysis. 2. Effect of NOx Concentration. *Environ. Sci. Technol.* **2005**, *39*, 7046−7054.
(44) Gibilisco, R. G.; Blanco, M. B.; Bejan, I.; Barnes, I.; Wiesen, P.; Teruel, M. A. Atmospheric Sink of (E)-3-Hexen-1-ol, (Z)-3-Hepten-1-ol, and (Z)-3-Octen-1-ol: Rate Coefficients and Mechanisms of the OH-Radical Initiated Degradation. *Environ. Sci. Technol.* **2015**, *49*, 7717−7725.
(45) Joutsensaari, J.; Yli-Pirilä, P.; Korhonen, H.; Arola, A.; Blande, J. D.; Heijari, J.; Kivimäenpää, M.; Mikkonen, S.; Hao, L.; Miettinen, P.; Lyytikäinen-Saarenmaa, P.; Faiola, C. L.; Laaksonen, A.; Holopainen, J. K. Biotic stress accelerates formation of climate-relevant aerosols in boreal forests. *Atmos. Chem. Phys.* **2015**, *15*, 12139−12157.
(46) Trimm, H. H.; Hunter, W., *Industrial Chemistry: New Applications, Processes and Systems*; Apple Academic Press, 2016.
(47) Heiden, A. C.; Kobel, K.; Komenda, M.; Koppmann, R.; Shao, M.; Wildt, J. Toluene emissions from plants. *Geophys. Res. Lett.* **1999**, *26*, 1283−1286.
(48) Horie, O.; Moortgat, G. K. Gas-Phase Ozonolysis of Alkenes. Recent Advances in Mechanistic Investigations. *Acc. Chem. Res.* **1998**, *31*, 387−396.
(49) Richards-Henderson, N. K.; Hansel, A. K.; Valsaraj, K. T.; Anastasio, C. Aqueous oxidation of green leaf volatiles by hydroxyl radical as a source of SOA: Kinetics and SOA yields. *Atmos. Environ.* **2014**, *95*, 105−112.
(50) Atkinson, R.; Hasegawa, D.; Aschmann, S. M. Rate constants for the gas-phase reactions of O3 with a series of monoterpenes and related compounds at 296 ± 2 K. *Int. J. Chem. Kinet.* **1990**, *22*, 871−887.
(51) Dash, M. R.; Balaganesh, M.; Rajakumar, B. Rate coefficients for the gas-phase reaction of OH radical with α-pinene: an experimental and computational study. *Mol. Phys.* **2013**, *112*, 1495−1511.
(52) Presto, A. A.; Huff Hartz, K. E.; Donahue, N. M. Secondary Organic Aerosol Production from Terpene Ozonolysis. 1. Effect of UV Radiation. *Environ. Sci. Technol.* **2005**, *39*, 7036−7045.
(53) Hamilton, J. F.; Lewis, A. C.; Carey, T. J.; Wenger, J. C.; Borrás i Garcia, E.; Muñoz, A. Reactive oxidation products promote secondary organic aerosol formation from green leaf volatiles. *Atmos. Chem. Phys.* **2009**, *9*, 3815−3823.
(54) Odum, J. R.; Hoffmann, T.; Bowman, F.; Collins, D.; Flagan, R. C.; Seinfeld, J. H. Gas/Particle Partitioning and Secondary Organic Aerosol Yields. *Environ. Sci. Technol.* **1996**, *30*, 2580−2585.
(55) Yeh, G. K.; Ziemann, P. J. Alkyl Nitrate Formation from the Reactions of C8−C14 n-Alkanes with OH Radicals in the Presence of NOx: Measured Yields with Essential Corrections for Gas−Wall Partitioning. *J. Phys. Chem. A* **2014**, *118*, 8147−8157.
(56) Bian, Q.; May, A. A.; Kreidenweis, S. M.; Pierce, J. R. Investigation of particle and vapor wall-loss effects on controlled wood-smoke smog-chamber experiments. *Atmos. Chem. Phys.* **2015**, *15*, 11027−11045.
(57) Zaytsev, A.; Koss, A. R.; Breitenlechner, M.; Krechmer, J. E.; Nihill, K. J.; Lim, C. Y.; Rowe, J. C.; Cox, J. L.; Moss, J.; Roscioli, J. R.; Canagaratna, M. R.; Worsnop, D. R.; Kroll, J. H.; Keutsch, F. N. Mechanistic study of the formation of ring-retaining and ring-opening products from the oxidation of aromatic compounds under urban atmospheric conditions. *Atmos. Chem. Phys.* **2019**, *19*, 15117−15129.
(58) Zhang, X.; Cappa, C. D.; Jathar, S. H.; McVay, R. C.; Ensberg, J. J.; Kleeman, M. J.; Seinfeld, J. H. Influence of vapor wall loss in laboratory chambers on yields of secondary organic aerosol. *Proc. Natl. Acad. Sci.* **2014**, *111*, 5802−5807.
(59) Grosjean, E.; Grosjean, D. The gas-phase reaction of alkenes with ozone. *Atmos. Environ.* **1998**, *32*, 3393−3402.
(60) Aschmann, S. M.; Shu, Y.; Arey, J.; Atkinson, R. Products of the gas-phase reactions of cis-3-hexen-1-ol with OH radicals and O3. *Atmos. Environ.* **1997**, *31*, 3551−3560.
(61) Winterhalter, R.; Van Dingenen, R.; Larsen, B. R.; Jensen, N. R.; Hjorth, J. LC-MS analysis of aerosol particles from the oxidation of α-pinene by ozone and OH-radicals. *Atmos. Chem. Phys. Discuss.* **2003**, *3*, 1−39.
(62) Docherty, K. S.; Wu, W.; Lim, Y. B.; Ziemann, P. J. Contributions of Organic Peroxides to Secondary Aerosol Formed from Reactions of Monoterpenes with O3. *Environ. Sci. Technol.* **2005**, *39*, 4049−4059.
(63) Vereecken, L.; Francisco, J. S. Theoretical studies of atmospheric reaction mechanisms in the troposphere. *Chem. Soc. Rev.* **2012**, *41*, 6259−6293.
(64) Torres, A. L.; Buchan, H. Tropospheric nitric oxide measurements over the Amazon Basin. *J. Geophys. Res.: Atmos.* **1988**, *93*, 1396−1406.
(65) McFarland, M.; Kley, D.; Drummond, J. W.; Schmeltekopf, A. L.; Winkler, R. H. Nitric oxide measurements in the equatorial Pacific region. *Geophys. Res. Lett.* **1979**, *6*, 605−608.
(66) Tobias, H. J.; Ziemann, P. J. Thermal Desorption Mass Spectrometric Analysis of Organic Aerosol Formed from Reactions of 1-Tetradecene and O3 in the Presence of Alcohols and Carboxylic Acids. *Environ. Sci. Technol.* **2000**, *34*, 2105−2115.

https://dx.doi.org/10.1021/acsearthspacechem.0c00092
ACS Earth Space Chem. XXXX, XXX, XXX−XXX

(67) Mentel, T. F.; Springer, M.; Ehn, M.; Kleist, E.; Pullinen, I.; Kurtén, T.; Rissanen, M.; Wahner, A.; Wildt, J. Formation of highly oxidized multifunctional compounds: autoxidation of peroxy radicals formed in the ozonolysis of alkenes − deduced from structure−product relationships. *Atmos. Chem. Phys.* **2015**, *15*, 6745−6765.
(68) Tsao, C. C.; Campbell, J. E.; Mena-Carrasco, M.; Spak, S. N.; Carmichael, G. R.; Chen, Y. Increased estimates of air-pollution emissions from Brazilian sugar-cane ethanol. *Nat. Clim. Chang.* **2012**, *2*, 53−57.
(69) Agency, U. E. P., *Estimation Programs Interface Suite*. 4.11 ed.; Washington DC, USA, 2014.
(70) Chen, L.; Huang, Y.; Xue, Y.; Cao, J.; Wang, W. Effect of oligomerization reactions of Criegee intermediate with organic acid/peroxy radical on secondary organic aerosol formation from isoprene ozonolysis. *Atmos. Environ.* **2018**, *187*, 218−229.
(71) Chen, L.; Wang, W.; Wang, W.; Liu, Y.; Liu, F.; Liu, N.; Wang, B. Water-catalyzed decomposition of the simplest Criegee intermediate CH2OO. *Theor. Chem. Acc.* **2016**, *135*, 131.
(72) Long, B.; Tan, X.-f.; Long, Z.-w.; Wang, Y.-b.; Ren, D.-s.; Zhang, W.-j. Theoretical Studies on Reactions of the Stabilized H2COO with HO2 and the HO2···H2O Complex. *J. Phys. Chem. A* **2011**, *115*, 6559−6567.
(73) Nguyen, T. B.; Tyndall, G. S.; Crounse, J. D.; Teng, A. P.; Bates, K. H.; Schwantes, R. H.; Coggon, M. M.; Zhang, L.; Feiner, P.; Millller, D. O.; Skog, K. M.; Rivera-Rios, J. C.; Dorris, M.; Olson, K. F.; Koss, A.; Wild, R. J.; Brown, S. S.; Goldstein, A. H.; de Gouw, J. A.; Brune, W. H.; Keutsch, F. N.; Seinfeld, J. H.; Wennberg, P. O. Atmospheric fates of Criegee intermediates in the ozonolysis of isoprene. *Phys. Chem. Chem. Phys.* **2016**, *18*, 10241−10254.
(74) Zhang, X.; McVay, R. C.; Huang, D. D.; Dalleska, N. F.; Aumont, B.; Flagan, R. C.; Seinfeld, J. H. Formation and evolution of molecular products in α-pinene secondary organic aerosol. *Proc. Natl. Acad. Sci. U. S. A.* **2015**, *112*, 14168−14173.
(75) Inomata, S.; Sato, K.; Hirokawa, J.; Sakamoto, Y.; Tanimoto, H.; Okumura, M.; Tohno, S.; Imamura, T. Analysis of secondary organic aerosols from ozonolysis of isoprene by proton transfer reaction mass spectrometry. *Atmos. Environ.* **2014**, *97*, 397−405.
(76) Sakamoto, Y.; Inomata, S.; Hirokawa, J. Oligomerization Reaction of the Criegee Intermediate Leads to Secondary Organic Aerosol Formation in Ethylene Ozonolysis. *J. Phys. Chem. A* **2013**, *117*, 12912−12921.
(77) Kalberer, M.; Paulsen, D.; Sax, M.; Steinbacher, M.; Dommen, J.; Prévôt, A. S.; Fisseha, R.; Weingartner, E.; Frankevich, V.; Zenobi, R.; Baltensperger, U. Identification of Polymers as Major Components of Atmospheric Organic Aerosols. *Science* **2004**, *303*, 1659−1662.
(78) Jang, M.; Czoschke, N. M.; Lee, S.; Kamens, R. M. Heterogeneous Atmospheric Aerosol Production by Acid-Catalyzed Particle-Phase Reactions. *Science* **2002**, *298*, 814−817.
(79) Heaton, K. J.; Dreyfus, M. A.; Wang, S.; Johnston, M. V. Oligomers in the Early Stage of Biogenic Secondary Organic Aerosol Formation and Growth. *Environ. Sci. Technol.* **2007**, *41*, 6129−6136.
(80) Shen, H.; Chen, Z.; Li, H.; Qian, X.; Qin, X.; Shi, W. Gas-Particle Partitioning of Carbonyl Compounds in the Ambient Atmosphere. *Environ. Sci. Technol.* **2018**, *52*, 10997−11006.
(81) Perraud, V.; Bruns, E. A.; Ezell, M. J.; Johnson, S. N.; Yu, Y.; Alexander, M. L.; Zelenyuk, A.; Imre, D.; Chang, W. L.; Dabdub, D.; Pankow, J. F.; Finlayson-Pitts, B. J. Nonequilibrium atmospheric secondary organic aerosol formation and growth. *Proc. Natl. Acad. Sci. U. S. A.* **2012**, *109*, 2836−2841.
(82) O'Brien, R. E.; Neu, A.; Epstein, S. A.; MacMillan, A. C.; Wang, B.; Kelly, S. T.; Nizkorodov, S. A.; Laskin, A.; Moffet, R. C.; Gilles, M. K. Physical properties of ambient and laboratory-generated secondary organic aerosol. *Geophys. Res. Lett.* **2014**, *41*, 4347−4353.
(83) Power, R. M.; Simpson, S. H.; Reid, J. P.; Hudson, A. J. The transition from liquid to solid-like behaviour in ultrahigh viscosity aerosol particles. *Chem. Sci.* **2013**, *4*, 2597−2604.
(84) Shiraiwa, M.; Zuend, A.; Bertram, A. K.; Seinfeld, J. H. Gas−particle partitioning of atmospheric aerosols: interplay of physical state, non-ideal mixing and morphology. *Phys. Chem. Chem. Phys.* **2013**, *15*, 11441−11453.
(85) Kuwata, M.; Martin, S. T. Phase of atmospheric secondary organic material affects its reactivity. *Proc. Natl. Acad. Sci. U. S. A.* **2012**, *109*, 17354−17359.
(86) Pajunoja, A.; Lambe, A. T.; Hakala, J.; Rastak, N.; Cummings, M. J.; Brogan, J. F.; Hao, L.; Paramonov, M.; Hong, J.; Prisle, N. L.; Malila, J.; Romakkaniemi, S.; Lehtinen, K. E. J.; Laaksonen, A.; Kulmala, M.; Massoli, P.; Onasch, T. B.; Donahue, N. M.; Riipinen, I.; Davidovits, P.; Worsnop, D. R.; Petäjä, T.; Virtanen, A. Adsorptive uptake of water by semisolid secondary organic aerosols. *Geophys. Res. Lett.* **2015**, *42*, 3063−3068.
(87) Virtanen, A.; Kannosto, J.; Kuuluvainen, H.; Arffman, A.; Joutsensaari, J.; Saukko, E.; Hao, L.; Yli-Pirilä, P.; Tiitta, P.; Holopainen, J. K.; Keskinen, J.; Worsnop, D. R.; Smith, J. N.; Laaksonen, A. Bounce behavior of freshly nucleated biogenic secondary organic aerosol particles. *Atmos. Chem. Phys.* **2011**, *11*, 8759−8766.
(88) Slade, J. H.; Knopf, D. A. Multiphase OH oxidation kinetics of organic aerosol: The role of particle phase state and relative humidity. *Geophys. Res. Lett.* **2014**, *41*, 5297−5306.
(89) Slade, J. H.; Shiraiwa, M.; Arangio, A.; Su, H.; Pöschl, U.; Wang, J.; Knopf, D. A. Cloud droplet activation through oxidation of organic aerosol influenced by temperature and particle phase state. *Geophys. Res. Lett.* **2017**, *44*, 1583−1591.
(90) Bateman, A. P.; Bertram, A. K.; Martin, S. T. Hygroscopic Influence on the Semisolid-to-Liquid Transition of Secondary Organic Materials. *J. Phys. Chem. A* **2014**, *119*, 4386−4395.
(91) Pajunoja, A.; Hu, W.; Leong, Y. J.; Taylor, N. F.; Miettinen, P.; Palm, B. B.; Mikkonen, S.; Collins, D. R.; Jimenez, J. L.; Virtanen, A. Phase state of ambient aerosol linked with water uptake and chemical aging in the southeastern US. *Atmos. Chem. Phys.* **2016**, *16*, 11163−11176.
(92) Saukko, E.; Kuuluvainen, H.; Virtanen, A. A method to resolve the phase state of aerosol particles. *Atmos. Meas. Tech.* **2012**, *5*, 259−265.
(93) Renbaum-Wolff, L.; Grayson, J. W.; Bateman, A. P.; Kuwata, M.; Sellier, M.; Murray, B. J.; Shilling, J. E.; Martin, S. T.; Bertram, A. K. Viscosity of α-pinene secondary organic material and implications for particle growth and reactivity. *Proc. Natl. Acad. Sci.* **2013**, *110*, 8014−8019.
(94) Sakamoto, Y.; Yajima, R.; Inomata, S.; Hirokawa, J. Water vapour effects on secondary organic aerosol formation in isoprene ozonolysis. *Phys. Chem. Chem. Phys.* **2017**, *19*, 3165−3175.
(95) Hinks, M. L.; Montoya-Aguilera, J.; Ellison, L.; Lin, P.; Laskin, A.; Laskin, J.; Shiraiwa, M.; Dabdub, D.; Nizkorodov, S. A. Effect of relative humidity on the composition of secondary organic aerosol from the oxidation of toluene. *Atmos. Chem. Phys.* **2018**, *18*, 1643−1652.
(96) Warren, B.; Malloy, Q. G. J.; Yee, L. D.; Cocker, D. R., III Secondary organic aerosol formation from cyclohexene ozonolysis in the presence of water vapor and dissolved salts. *Atmos. Environ* **2009**, *43*, 1789−1795.
(97) Hennigan, C. J.; Bergin, M. H.; Dibb, J. E.; Weber, R. J. Enhanced secondary organic aerosol formation due to water uptake by fine particles. *Geophys. Res. Lett.* **2008**, *35*, L18801.
(98) Jathar, S. H.; Mahmud, A.; Barsanti, K. C.; Asher, W. E.; Pankow, J. F.; Kleeman, M. J. Water uptake by organic aerosol and its influence on gas/particle partitioning of secondary organic aerosol in the United States. *Atmos. Environ.* **2016**, *129*, 142−154.
(99) Booth, A. M.; Murphy, B.; Riipinen, I.; Percival, C. J.; Topping, D. O. Connecting Bulk Viscosity Measurements to Kinetic Limitations on Attaining Equilibrium for a Model Aerosol Composition. *Environ. Sci. Technol.* **2014**, *48*, 9298−9305.
(100) Cappa, C. D.; Wilson, K. R. Evolution of organic aerosol mass spectra upon heating: implications for OA phase and partitioning behavior. *Atmos. Chem. Phys.* **2011**, *11*, 1895−1911.
(101) Vaden, T. D.; Imre, D.; Beranek, J.; Shrivastava, M.; Zelenyuk, A. Evaporation kinetics and phase of laboratory and ambient

https://dx.doi.org/10.1021/acsearthspacechem.0c00092
ACS Earth Space Chem. XXXX, XXX, XXX−XXX

secondary organic aerosol. *Proc. Natl. Acad. Sci. U. S. A.* **2011**, *108*, 2190−2195.
(102) Abramson, E.; Imre, D.; Beránek, J.; Wilson, J.; Zelenyuk, A. Experimental determination of chemical diffusion within secondary organic aerosol particles. *Phys. Chem. Chem. Phys.* **2013**, *15*, 2983−2991.
(103) Zaveri, R. A.; Shilling, J. E.; Zelenyuk, A.; Zawadowicz, M. A.; Suski, K.; China, S.; Bell, D. M.; Veghte, D.; Laskin, A. Particle-Phase Diffusion Modulates Partitioning of Semivolatile Organic Compounds to Aged Secondary Organic Aerosol. *Environ. Sci. Technol.* **2020**, *54*, 2595−2605.
(104) Riipinen, I.; Pierce, J. R.; Yli-Juuti, T.; Nieminen, T.; Häkkinen, S.; Ehn, M.; Junninen, H.; Lehtipalo, K.; Petäjä, T.; Slowik, J.; Chang, R.; Shantz, N. C.; Abbatt, J.; Leaitch, W. R.; Kerminen, V. M.; Worsnop, D. R.; Pandis, S. N.; Donahue, N. M.; Kulmala, M. Organic condensation: a vital link connecting aerosol formation to cloud condensation nuclei (CCN) concentrations. *Atmos. Chem. Phys.* **2011**, *11*, 3865−3878.
(105) Shiraiwa, M.; Ammann, M.; Koop, T.; Poschl, U. Gas uptake and chemical aging of semisolid organic aerosol particles. *Proc. Natl. Acad. Sci. U. S. A.* **2011**, *108*, 11003−11008.
(106) Zaveri, R. A.; Shilling, J. E.; Zelenyuk, A.; Liu, J.; Bell, D. M.; D'Ambro, E. L.; Gaston, C. J.; Thornton, J. A.; Laskin, A.; Lin, P.; Wilson, J.; Easter, R. C.; Wang, J.; Bertram, A. K.; Martin, S. T.; Seinfeld, J. H.; Worsnop, D. R. Growth Kinetics and Size Distribution Dynamics of Viscous Secondary Organic Aerosol. *Environ. Sci. Technol.* **2018**, *52*, 1191−1199.
(107) Shilling, J. E.; Chen, Q.; King, S. M.; Rosenoern, T.; Kroll, J. H.; Worsnop, D. R.; DeCarlo, P. F.; Aiken, A. C.; Sueper, D.; Jimenez, J. L.; Martin, S. T. Loading-dependent elemental composition of α-pinene SOA particles. *Atmos. Chem. Phys.* **2009**, *9*, 771−782.
(108) Grayson, J. W.; Zhang, Y.; Mutzel, A.; Renbaum-Wolff, L.; Böge, O.; Kamal, S.; Herrmann, H.; Martin, S. T.; Bertram, A. K. Effect of varying experimental conditions on the viscosity of α-pinene derived secondary organic material. *Atmos. Chem. Phys.* **2016**, *16*, 6027−6040.

https://dx.doi.org/10.1021/acsearthspacechem.0c00092
ACS Earth Space Chem. XXXX, XXX, XXX−XXX